

See discussions, stats, and author profiles for this publication at: <https://www.researchgate.net/publication/265732372>

Synthesis, Characterization of Some Ferrocenoyl Cysteine and Histidine Conjugates, and Their Interactions with Some Metal Ions

ARTICLE *in* BERICHTE DER DEUTSCHEN CHEMISCHEN GESELLSCHAFT · NOVEMBER 2014

Impact Factor: 2.94 · DOI: 10.1002/ejic.201402470

READS

18

5 AUTHORS, INCLUDING:



Guo-Cheng Han

Guilin University of Electronic Technology

17 PUBLICATIONS 44 CITATIONS

SEE PROFILE



Heinz Bernhard Kraatz

University of Toronto

308 PUBLICATIONS 5,495 CITATIONS

SEE PROFILE

DOI:10.1002/ejic.201402470

Synthesis, Characterization of Some Ferrocenoyl Cysteine and Histidine Conjugates, and Their Interactions with Some Metal Ions

Guo-Cheng Han,^{[a],‡} Annaleizle Ferranco,^{[b],‡} Xiao-Zhen Feng,^[a]
Zhencheng Chen,^{*[a]} and Heinz-Bernhard Kraatz^{*[b]}

Keywords: Bioinorganic chemistry / Metallocenes / Cysteine / Histidine / Peptides

The synthesis and characterization of a series of 1,*n*'-disubstituted ferrocenoyl cysteine and histidine conjugates is reported. Their interaction with a range of metal ions was studied. The results show that metal coordination in His-con-

taining peptides involved the imidazole group. Metal coordination affects the structural properties of the ferrocene (Fc) conjugates, as judged by CD spectroscopy, and also the redox properties of the Fc group.

Introduction

Cysteine (Cys) as part of peptides and proteins can serve as a nucleophile in enzymatic reactions^[1] or as a redox-active group resulting in the formation of cystine, a disulfide,^[2] and is widely involved in metal coordination, giving rise to a wide range of metalloproteins that play a critical role in various biological processes. Examples are the FeMo-cofactor in nitrogenase, in which the metal cluster is linked to the protein via cysteine thiols,^[3] or other Fc-S clusters,^[4–7] which play important roles in electron transfer reactions, such as aerobic respiration, photosynthesis, and biodegradation of various alkene and aromatic compounds. Examples of other metalloproteins involving metal coordination to Cys include the Zn^{II} in zinc finger protein^[8] and alcohol dehydrogenase, the Cu present in blue copper,^[9] Fe in cytochrome P450,^[10] and Ni in the NiFe-hydrogenases.^[11]

The thiol group also has a high affinity for toxic heavy metals including Hg²⁺, Pb²⁺, Cd²⁺,^[12] and has, for example, enabled the removal of Pb²⁺ from dithiocarbamate-capped Ag nanoparticles.^[13] Jalilehvand and co-workers^[14–17] have investigated the potential for Hg²⁺ complex formation with Cys and other thiolate-containing biological molecules at both physiological and alkaline pH, with the aim of

developing an understanding towards detoxification and removal of Hg upon exposure. Cd^{II} has serious effects on human health, causing damage to kidneys and lungs, and triggers bone diseases and potentially leads to cancer.^[18,19] Although the Cd^{II} ion is slightly larger than Zn^{II} (0.78 Å vs. 0.6 Å in tetrahedral geometry),^[20] it is able to bind to the Cys thiol with high affinity, interrupting biological events.^[21,22] This has led to further research focusing on the development of chelating agents to prevent the uptake of Cd^{II} by cells.^[23–26] The structural similarity of Cd²⁺ to Zn²⁺ has prompted thorough comparisons of the coordination properties of the two ions and studies of the metal selectivity for Zn²⁺, for example, in mammalian metal transporters, such as zinc influx transporters.^[27] Zn²⁺ also plays many significant roles in physiological systems. For example, it is present in the catalytic site of carbonic anhydrase, a metalloenzyme with three histidine (His) residues coordinated to the zinc ion, and it is also present in structural sites such as the zinc finger protein.^[28–30]

Additional work involving the coordination chemistry of Cys with other metals including Bi³⁺ has been reported.^[31,32] The use of Bi for treatment of diseases and disorders has motivated researchers to direct their attention towards characterization of bismuth–thiolate complexes to understand its therapeutic use and efficacy.^[33,34] Burford and colleagues have shown that reactions of Bi(NO₃)₃ with L-cysteine, jointly with other amino acids, lead to a wide range of new biologically important complex ions of Bi³⁺ that provide a valuable understanding of the bioactivity of Bi³⁺.^[35]

Other ongoing research regarding complex formation between Cys and metals includes coordination studies with Ag^I. Exploration into this area of study has grown as a result of the increased resistance of bacteria towards antibiotics.^[36–38] A better grasp of the fundamental structure

[a] School of Life and Environmental Sciences, Guilin University of Electronic Technology, Guilin 541004, P. R. China
E-mail: chenzhcheng@163.com
<http://rsc.guet.edu.cn/RSC/public/show.aspx?par2=0014&par=864>

[b] Department of Physical and Environmental Sciences, University of Toronto Scarborough, Toronto, Ontario M1C 1A4, Canada
E-mail: bernie.kraatz@utoronto.ca
<http://www.utsc.utoronto.ca/~bkraatz/>

[‡] Both authors contributed to this manuscript equally
Supporting information for this article is available on the WWW under <http://dx.doi.org/10.1002/ejic.201402470>.

and mechanism of the coordination of Ag^{I} with Cys, other sulfur-containing amino acids, and their derivatives is crucial to creating a broader view of the antimicrobial activity of silver ions, including their influence on bacterial activity in the environment; these are all very important properties for developing more functional antimicrobial Ag^{I} compounds. A recent study investigated complex formation between Ag^{I} and cysteine, penicillamine, and glutathione in alkaline aqueous solution, exploring complexation by extended X-ray absorption fine structure and ^{109}Ag NMR spectroscopic measurements.^[39]

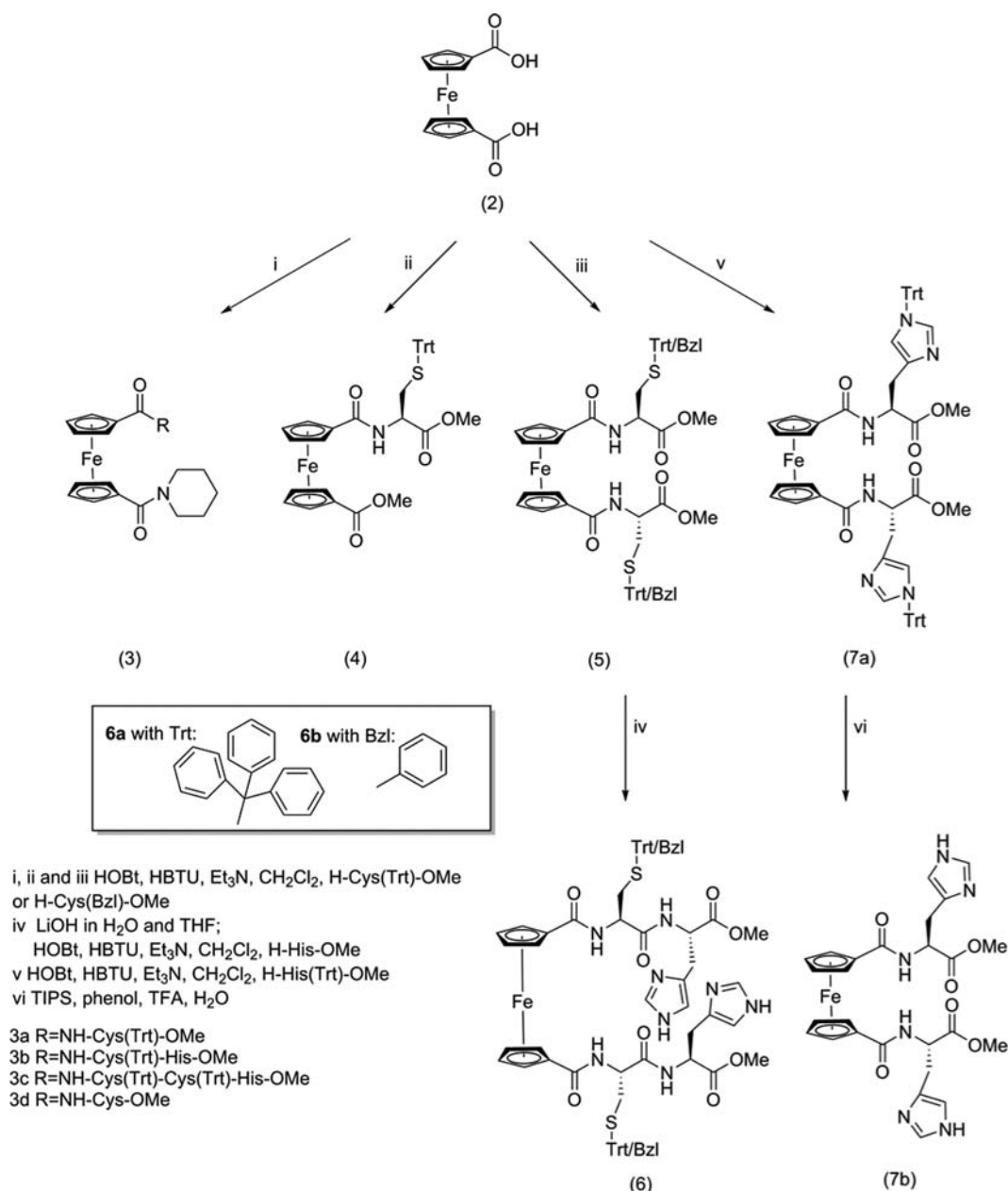
Ferrocene (Fc) has been recognized as an organometallic scaffold that allows templating of peptide secondary structures largely due to a favorable inter-ring spacing, and a wide range of Fc bioconjugates have been reported that dis-

play a fascinating array of well-defined H-bonded structures.^[40] And while some examples of metal coordination to Fc peptide have been described in the literature,^[41] detailed coordination studies of His- and Cys-containing Fc conjugates with metal ions and their effect on redox properties have not been reported. Here, we report the synthesis and characterization of Fc conjugates of Cys and His together with their metal coordination behavior and its effect on electrochemical properties.

Results and Discussion

Synthesis and Characterization

The synthetic strategy of Fc-Cys and Fc-His derivatives is shown in Scheme 1. For compounds **3a** and **3b**, the cou-



Scheme 1. Synthesis of ferrocenoyl amino acid and peptide derivatives.

pling strategies involve 1,*n*'-ferrocene dicarboxylic acid Fc[COOH]₂ (**2**), HOBt, and HBTU as coupling reagents, and the deprotected Fmoc group of dipeptide Fmoc-Cys(Trt)-His-OMe (**1**). Here we use the Fmoc protecting group instead of the Boc protecting group on the amine, because of the orthogonality of the two protection schemes, and as we wanted to avoid problems related to the concomitant removal of the Boc and trityl group under acidic conditions. The synthetic procedure of compound **3c** is similar to that of compound **3b**.

The ¹H NMR spectra of the Fc-Cys and Fc-His derivatives are shown in Figure S1 (Supporting Information), and pertinent ¹H NMR spectroscopic data is summarized in Table 1.

Table 1. Summary of the ¹H NMR spectroscopic parameters (δ values in ppm) for Fc amino acid conjugates **4**, **5**, **6a**, **6b**, **7a**, and **7b**, each prepared at a concentration of 1 mM in CDCl₃ or [D₃]acetonitrile.^[a]

| Cpd. | Amide-NH | Trt | CH-Cys | CH ₂ -Cys | CH-His | CH ₂ -His |
|--------------------------|----------|-----------|--------|----------------------|--------|----------------------|
| 3a | 9.17 | 7.46–7.20 | 4.36 | 2.86–2.60 | – | – |
| 3b | 9.75 | 7.50–7.17 | 2.90 | 2.75–2.70 | 4.71 | 3.20–3.00 |
| 3c | 9.30 | 7.10–7.15 | 4.01 | 2.83–2.55 | 4.60 | 3.12–2.98 |
| 3d | 9.48 | – | 4.33 | 3.08–3.03 | – | – |
| 4 | 6.49 | 7.42–7.19 | 4.73 | 2.74 | – | – |
| 5 | 7.52 | 7.37–7.16 | 4.70 | 2.76–2.47 | – | – |
| 6a | 8.36 | 7.45–7.13 | 3.15 | 1.26 | 3.15 | 3.20 |
| 6b | 8.54 | – | 4.77 | 3.22–2.65 | 4.77 | 3.22–2.65 |
| 7a | 7.87 | 7.28–7.19 | – | – | 4.92 | 3.21–2.63 |
| 7a ^[b] | 8.07 | 7.41–7.11 | – | – | 4.61 | 2.93 |
| 7b ^[b] | 7.89 | – | – | – | 4.94 | 3.47–3.24 |

[a] ¹H NMR spectroscopy at 1 mM concentration in [D]chloroform.
[b] ¹H NMR spectroscopy at 1 mM concentration in [D₃]acetonitrile because of solubility issues in chloroform.

Amide NH shifts for conjugates **3a–c** were observed in the 10–9 ppm range (δ = 9.17, 9.75, 9.30 ppm for compounds **3a**, **3b**, **3c**, respectively), suggesting their involvement in H-bonding, as their chemical shift is well above 7.00 ppm.^[42] Presumably, H-bonding interactions exist with the piperidine N on the other Cp ring of the Fc group. Upon deprotection of the Cys-S with trifluoroacetic acid (TFA), dithiothreitol (DTT), triethylsilane (TIS), and water, the isolated product **3d** lacks the resonances due to the trityl protecting group, while the amide H shift moves from 9.17 to 9.48 ppm (Figure S1B). Importantly, removal of the trityl group from the Cys-S for compounds **3b**, **3c**, **6a**, and **6b** was not successful. Potentially, steric effects due to the presence of the piperidine ring in conjugates **3a–c** were responsible for a lack of deprotection. We thus moved to an alternative strategy, in which Fc conjugates **4** and **5** were synthesized first (Scheme 1). A comparison of the amide NH resonances indicates that the amide NH for compound **4** is presumably not involved in H-bonding, since it is observed at δ = 6.49 ppm, while that of conjugate **5** is observed at δ = 7.52 ppm, which indicates the presence of H-bonding. Ester deprotection of Cys conjugate **5** with LiOH in THF was followed by coupling of the His group to form the conjugates Fc[CO-Cys(Trt)-His-OMe]₂ (**6a**) and Fc[CO-Cys(Bzl)-His-OMe]₂ (**6b**). Synthesis of Fc[CO-His(Trt)-OMe] (**7a**)

was achieved by direct coupling of 1,*n*'-ferrocene dicarboxylic acid Fc[COOH]₂ (**2**) with H-His(Trt)-OMe. The imidazole group of conjugate **7a** was deprotected with TFA in the presence of a silane and phenol to prevent the decomposition of the Fc group, which resulted in the clean formation of conjugate **7b**. The ¹H NMR spectra of conjugates **7a** and **7b** (Figure S1E) show amide signals (δ = 8.07 ppm for **7a** and δ = 7.89 ppm for **7b** in [D₃]MeCN) that are indicative of H-bonding interactions.^[43]

Circular dichroism (CD) studies were also carried out, which provide information about the helical chirality of the central Fc group. The CD spectra of Fc derivatives **3a–d** in acetonitrile solution at a concentration of 1 mM are shown in Figure S2 (Supporting Information). For each of the conjugates, a positive CD signal is observed with a maximum around 480 nm, indicating *P*-helical conformation for conjugates **3a–d**. Most L-amino acid conjugates of Fc, with exception of L-Cys, have *P*-helicity, while D-amino acid conjugates possess *M*-helicity.^[44] Herrick and co-workers reported a 1,2'-*P*-helical structure for disubstituted amino acid conjugates of Fc.^[45] This conformation is stabilized by H-bonds between the two podant amino acid substituents.^[45] It can be identified by CD spectra that *P*-helical conformation will exhibit a positive Cotton effect while *M*-helical conformation will display a negative Cotton effect at 480 nm. These CD properties of this Fc-centered CD signal are similar to that of a wide range of bis-peptide-substituted Fc derivatives of L-amino acids.^[40b,46]

Next, the redox properties of the Fc conjugates were examined by cyclic voltammetry (CV) by using tetrabutylammonium perchlorate (TBAP) as supporting electrolyte. Figure S3 (Supporting Information) shows a typical voltammogram at a scan rate of 100 mV s⁻¹. All conjugates display a single one-electron oxidation with half-wave potential ($E_{1/2}$) between 695 and 900 mV, and peak separations (ΔE) that are close to or under 100 mV (Tables 2 and 3). Piperidine conjugates **3a–d** exhibit oxidation potentials (659–776 mV) that are lower than those of the ester (**4**: $E_{1/2}$ = 859 mV) and the bis(amino acid) or bis(peptide) derivatives (839–901 mV).

Table 2. Electrochemical data obtained from CV of Fc amino acid conjugates **3a–d** in acetonitrile solution at a scan rate of 100 mV containing 0.1 M TBAP as supporting electrolyte. Potentials are given vs. Ag/AgCl.

| | $E_{1/2}$ (mV) | ΔE_p (mV) | i_{pa}/i_{pc} |
|-----------|----------------|-------------------|-----------------|
| 3a | 695 | 75 | 0.92 |
| 3d | 701 | 96 | 0.82 |
| 3b | 715 | 67 | 0.41 |
| 3c | 776 | 74 | 0.53 |

Peak separations for all conjugates are clearly larger than expected; it is also noteworthy that the ratios of the cathodic and anodic currents deviate from unity, which indicates quasi-reversibility of the electrochemical process. For compounds **3b** and **3c**, the ratios are 0.41 and 0.53, respectively.

Table 3. Electrochemical data obtained from CV of Fc amino acid conjugates **4**, **5**, **6a**, **6b**, **7a**, and **7b** in acetonitrile solution at a scan rate of 100 mV containing 0.1 M TBAP as supporting electrolyte vs. Ag/AgCl in the absence and presence of added metal ions.

| | No metal | | | Fe ^{II} | | | Zn ^{II} | | |
|--------------------------|-----------|--------------|-----------------|------------------|--------------|-----------------|------------------|--------------|-----------------|
| | $E_{1/2}$ | ΔE_p | i_{pa}/i_{pc} | $E_{1/2}$ | ΔE_p | i_{pa}/i_{pc} | $E_{1/2}$ | ΔE_p | i_{pa}/i_{pc} |
| | (mV) | (mV) | | (mV) | (mV) | | (mV) | (mV) | |
| 4 | 859 | 103 | 0.72 | 880 | 87 | 0.31 | 845 | 95 | 0.78 |
| 5 | 839 | 79 | 0.88 | 852 | 86 | 0.44 | 833 | 76 | 0.87 |
| 6a | 858 | 108 | 0.45 | 909 | 84 | 0.73 | 879 | 88 | 0.82 |
| 6b | 819 | 93 | 0.71 | 872 | 75 | 0.91 | 851 | 85 | 0.89 |
| 7a ^[a] | 837 | 74 | 0.89 | 839 | 111 | 0.77 | 835 | 162 | 0.61 |
| 7b ^[b] | 901 | 77 | 0.70 | 911 | 72 | 0.87 | 908 | 117 | 0.76 |

[a] CV was also used to study the interaction of **7a** with Cd²⁺: the $E_{1/2}$, ΔE_p , and i_{pa}/i_{pc} were 886 mV, 115 mV, and 0.76, respectively.
[b] CV was also used to study the interaction of **7b** with Cd²⁺: the $E_{1/2}$, ΔE_p , and i_{pa}/i_{pc} were 904 mV, 83 mV, and 0.82, respectively.

Interactions with Metal Ions

We probed the interactions of the Fc conjugates with metal ions. In order to probe these interactions, a series of ¹H NMR spectroscopic titrations, CD spectroscopic, mass

spectrometric, and electrochemical studies were conducted. NMR spectroscopic titrations are sensitive and can provide information about the coordination site and complex stoichiometry. Chemical shift variations can be observed as a result of metal coordination to specific amino acids.

First, NMR spectroscopic titrations were carried out for conjugates **7a** and **7b** as a function of added Cd²⁺, Zn²⁺, and Fe²⁺. The ¹H NMR spectra for the additions of Cd²⁺ to a solution of **7a** in CD₃CN are shown in Figure 1. Additions of Fe²⁺ and Zn²⁺ to a solution of **7a** and **7b** in CD₃CN are found in the Supporting Information. Figure 2 shows the ¹H NMR spectra for the additions of Cd²⁺ to a solution of **7b** in CD₃CN. As the chemical shifts of conjugates **7a** and **7b** were examined as a function of added metal ion Cd²⁺, it is observed that the signals of the imidazole protons δ and ϵ are changed by the addition of each metal ion. It is also noted that the amide proton appears to be affected by the addition of metal ions, as observed in Figures 3 and 4 for compounds **7a** and **7b**, correspondingly. Similar results were observed for the addition of the other transition metal ions to solutions of **7a** and **7b**, which is indicative of metal coordination involving the imidazole group of His. A plot of the chemical shift change ($\Delta\delta$) vs.

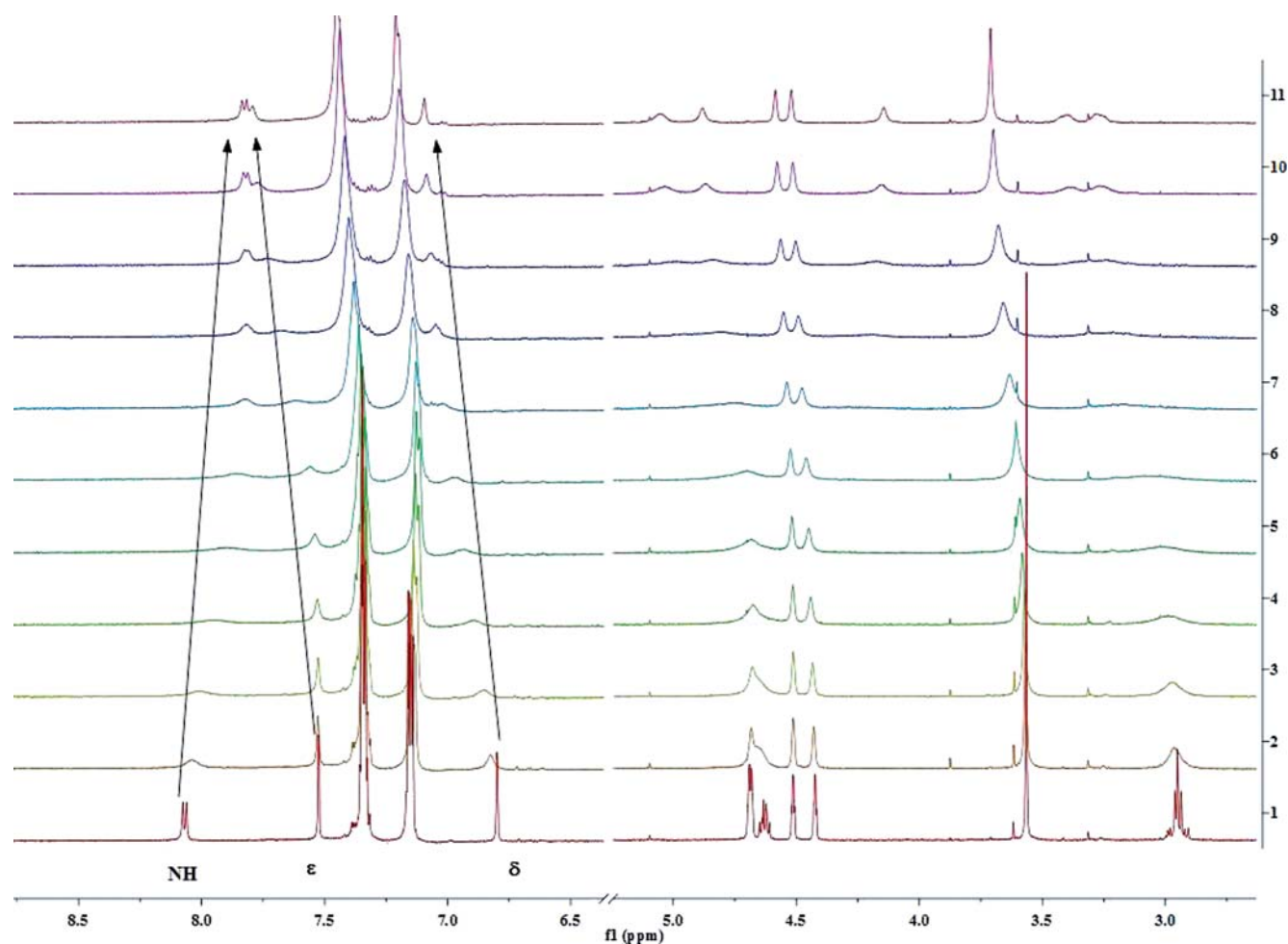


Figure 1. ¹H NMR spectroscopic titration experiments of conjugate **7a** with Cd²⁺. Ion Cd²⁺ was added at 0.0, 0.1, 0.2, 0.3, 0.4, 0.5, 0.6, 0.7, 0.8, 0.9, and 1.0 equiv. (shown from bottom to top) at a concentration of 1 mM for **7a** in CD₃CN.

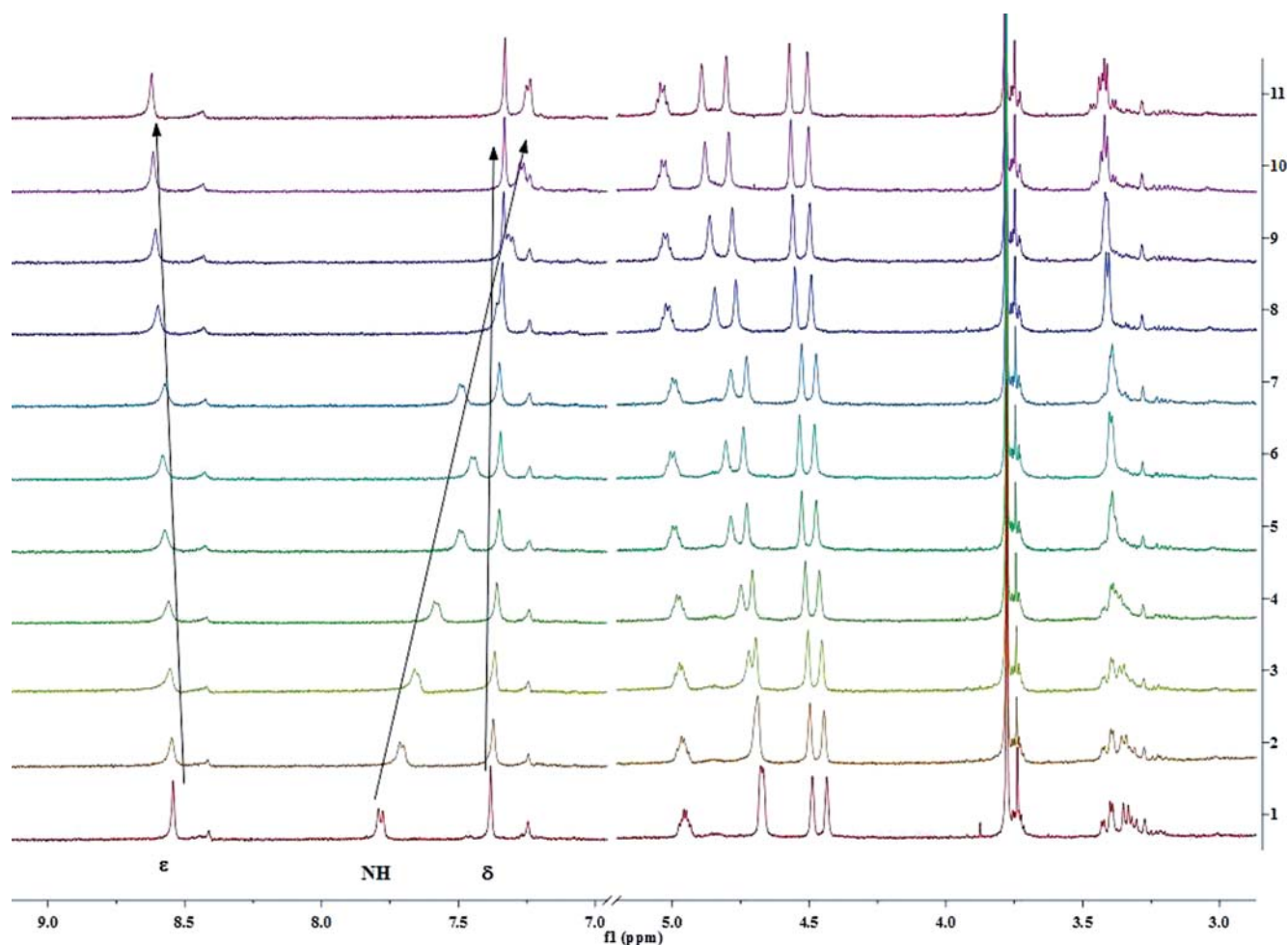


Figure 2. ^1H NMR spectroscopic titration experiments of conjugate **7b** with Cd^{2+} . Ion Cd^{2+} was added at 0.0, 0.1, 0.2, 0.3, 0.4, 0.5, 0.6, 0.7, 0.8, 0.9, and 1.0 equiv. (shown from bottom to top) at a concentration of 1 mM for **7b** in CD_3CN .

the equivalents of Zn^{2+} and Fe^{2+} added to the solution is shown in Figures S21 and S22, separately. Effectively, the results show that the chemical shift is affected until 1 equiv. of metal ion is added. Further addition of metal ion, such that the metal ion is in excess, does not cause any notable change to the chemical shifts. Our NMR spectroscopic ti-

trations indicate (a) a 1:1 stoichiometry with conjugates **7a** and **7b**, presumably, and (b) that coordination involves metal coordination to the imidazole N.

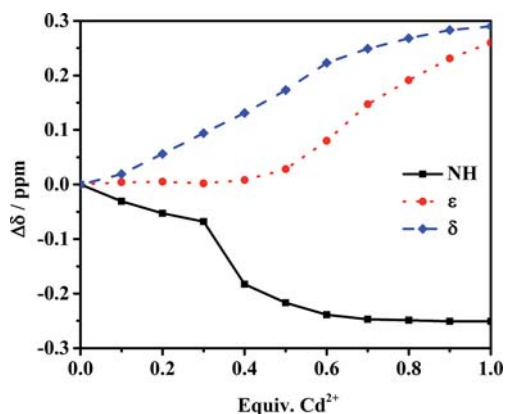


Figure 3. Changes in the chemical shifts of the amide proton, two His protons ϵ and δ as a function of Cd^{2+} added to a 1 mM solution of **7a** in CD_3CN .

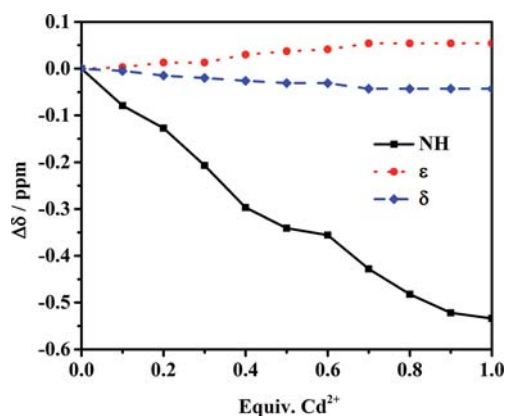


Figure 4. Changes in the chemical shifts of the amide proton, two His protons ϵ and δ as a function of Cd^{2+} added to a 1 mM solution of **7b** in CD_3CN .

We then carried out studies by CD spectroscopy, in which the effect of metal coordination on the helicity of the Fc core is studied. Figure 5 shows the CD spectra of

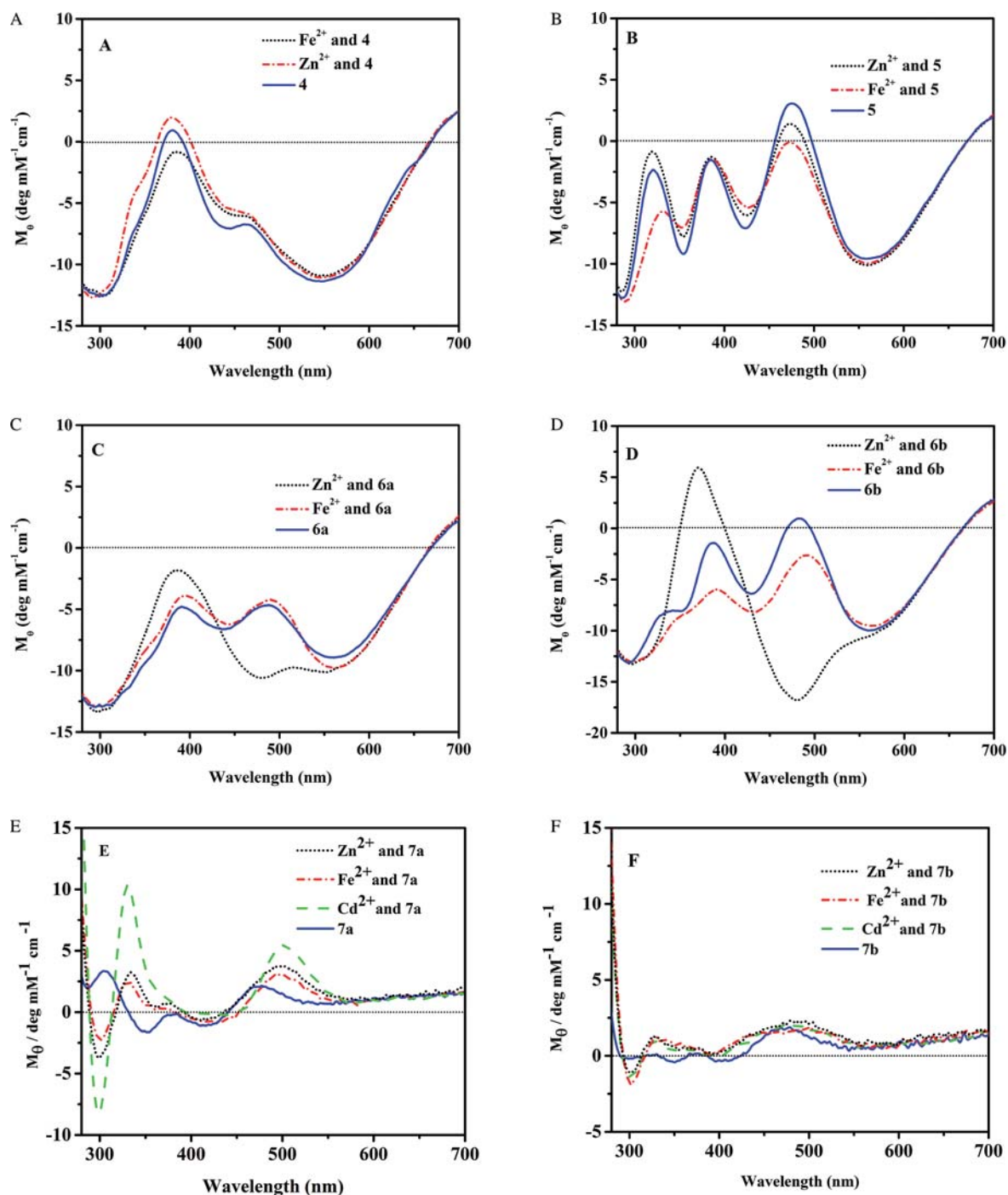


Figure 5. CD spectra of 1 mM of **4** (A), **5** (B), **6a** (C), **6b** (D), **7a** (E), and **7b** (F) in the absence of metal ions and in the presence of 1 equiv. of Fe^{2+} and 1 equiv. Zn^{2+} metal in acetonitrile. The CD spectra of **7a** and **7b** were also recorded with 1 equiv. Cd^{2+} metal (E and F, respectively).

compounds **4**, **5**, **6a**, **6b**, **7a**, and **7b** (1 mM in acetonitrile) in the absence and presence of equimolar amounts of Zn^{2+} and Fe^{2+} . In addition, studies were carried out for conjugates **7a** and **7b** with Cd^{2+} .

The CD spectra of conjugates **4** and **5** (Figure 5) remain virtually unchanged before and after the addition of Zn^{2+} and Fe^{2+} . In contrast, the CD spectra for compounds **6a** and **6b** are altered drastically upon addition of Zn^{2+} , while the addition of Fe^{2+} has no significant effect on the CD

spectra. Upon Zn^{2+} coordination, the symmetrical band at 480 nm now displays a negative Cotton effect, which suggests that metal coordination causes a change in the axial chirality of the Fc group of the conjugate (Figures 5C and 5D).

Conjugates **7a** and **7b** (Figures 5E and 5F) exhibit CD signals in the Fc region showing a positive Cotton effect and a maximum absorbance at $\lambda = 480$ nm, which is indicative of a *P*-helical conformation around the Fc group. How-

ever, notable changes are observed at $\lambda = 350$ nm showing a negative Cotton effect and this signal can be justified in part by transitions involving the Cp and the Fe. As a result of the contributions from the trityl protecting group on the imidazole ring of the His moiety, the observed CD signal is more intense compared with those of other Fc peptide conjugates.^[47] Importantly, addition of metal ions does not alter the axial stereochemistry.

In order to probe the effect of metal coordination on the electrochemical properties of the Fc conjugates, CV studies were carried out for conjugates **4**, **5**, **6a**, **6b**, **7a**, and **7b** in acetonitrile solution in the presence of Zn^{2+} and Fe^{2+} and their electrochemical properties were compared to those of the free Fc conjugates. In addition, **7a** and **7b** were also studied in the presence of Cd^{2+} . Addition of Fe^{2+} to the solution of conjugates **4** and **7a** resulted in a significant de-

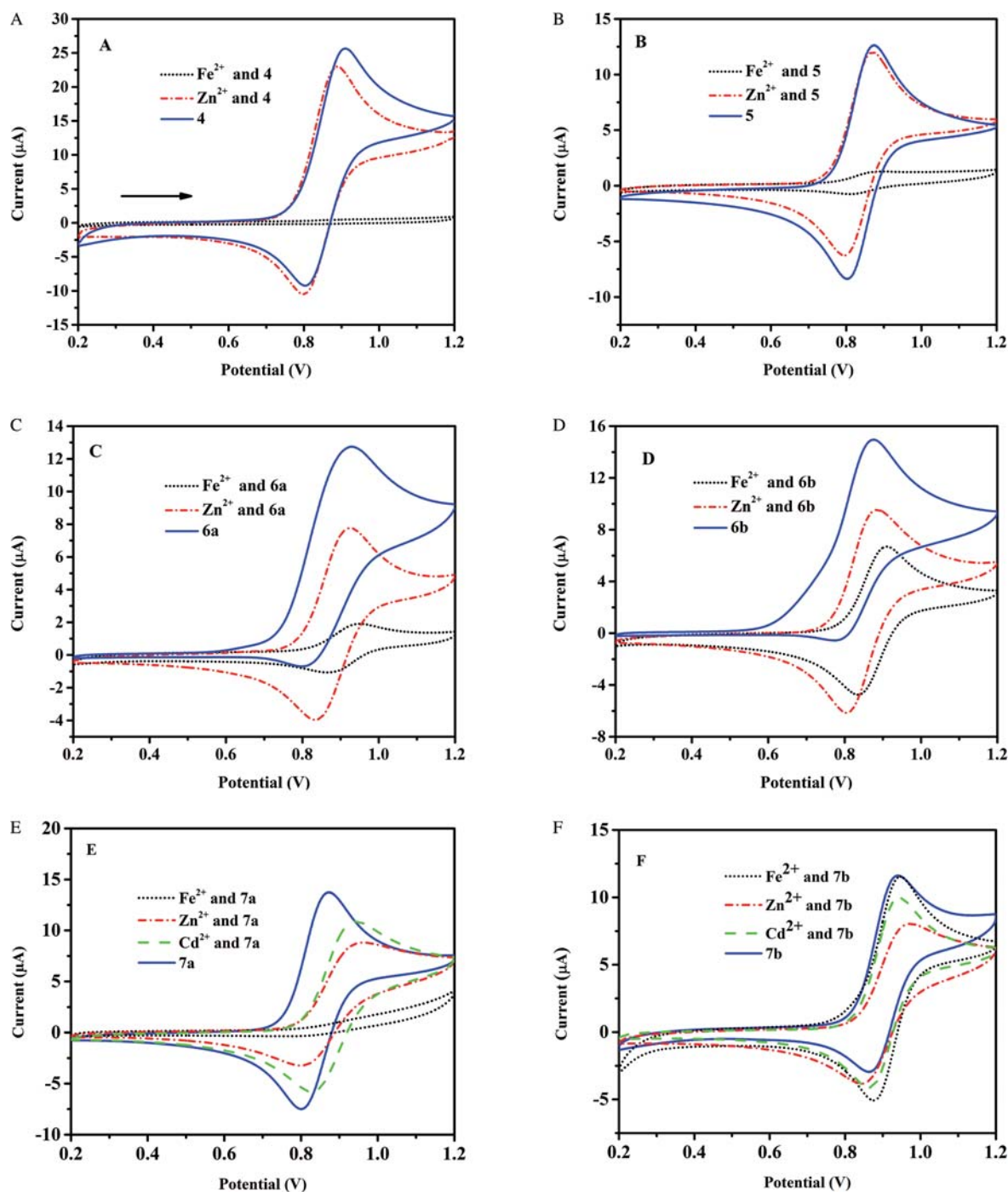


Figure 6. Cyclic voltammetry of **4** (A), **5** (B), **6a** (C), **6b** (D), **7a** (E), and **7b** (F) before and after the addition of 1 equiv. of Zn^{2+} and Fe^{2+} ions. The cyclic voltammetry plots of **7a** and **7b** were also recorded with 1 equiv. Cd^{2+} metal (E and F, respectively). Fc amino acid and peptide derivations had a concentration of 1 mM in acetonitrile; 0.1 M TBAP was added as supporting electrolyte; working electrode: glassy carbon, counter electrode: Pt wire, reference electrode: Ag/AgCl.

Table 4. Results of the high-resolution electrospray mass spectrometry analysis of acetonitrile solutions containing Fc conjugates **4**, **5**, **6a**, **6b**, **7a**, and **7b** in the absence and presence of Zn^{2+} .

| | No metal Mass | Calculated mass | Zn^{II} Mass | Calculated mass |
|--------------------------|-------------------------------------|-----------------|--|-----------------|
| 4 | 647.1385 $[\text{M}]^+$ | 647.1327 | 810.0678 $2[\text{M} - \text{Trt}]^+$ | 810.0667 |
| 5 | 993.2684 $[\text{M} + \text{H}]^+$ | 993.2616 | 508.0442 $[\text{M} - 2\text{Trt}]^+$ | 508.0425 |
| 6a | 1267.3835 $[\text{M} + \text{H}]^+$ | 1267.3843 | 845.0844 $[\text{M} - 2\text{Trt} + \text{Zn} + \text{H}]^+$ | 845.0817 |
| 6b | 963.2584 $[\text{M} + \text{H}]^+$ | 963.2621 | 1027.1815 $[\text{M} + \text{Zn} + \text{H}]^+$ | 1027.1912 |
| 7a ^[a] | 1061.3679 $[\text{M} + \text{H}]^+$ | 1061.3644 | 561.6424 $[\text{M} + \text{Zn}]^{2+}$ | 561.6408 |
| 7b ^[b] | 577.1438 $[\text{M} + \text{H}]^+$ | 577.1492 | 321.5342 $[\text{M} + \text{Zn}]^{2+}$ | 521.0429 |

[a] TOF-MS-ES⁺ (positive mode) of compound **7a** was also measured in the presence of Cd^{2+} , and the experimental and calculated masses $[\text{M} + \text{Cd}]^{2+}$ were 587.1339 and 587.1326, respectively. [b] TOF-MS-ES⁺ (positive mode) of compound **7b** was also measured in the presence of Cd^{2+} , and the experimental and calculated masses $[\text{M} + \text{Cd}]^{2+}$ were 345.0274 and 345.0300, respectively.

crease of the redox signal, most likely due to precipitation of the material or film formation on the surface, which prevented electron transfer. In case of **5**, **6a**, **6b**, and **7a**, the signal decreases, presumably as a result in changes of the diffusion of the complex to the electrode surface, and changes in the $E_{1/2}$ were observed. For **5**, **6a** and **6b**, the addition of Fe^{2+} causes shifts to higher potential are significant, while for **7a** and **7b** smaller anodic shifts are observed. The presence of Zn^{2+} and Cd^{2+} also causes small anodic shifts, suggesting that oxidation of the Fc group is more difficult after metal addition (Table 3 and Figure 6).

Electrospray ionization mass spectrometry is an ideal method to characterize metal coordination.^[48] The results of our mass spectrometric studies of Fc conjugates **4**, **5**, **6a**, **6b**, **7a**, and **7b** in the presence of equimolar amounts of Zn^{2+} are summarized in Table 4. Figure 7 shows the results of the MS experiments of complex formation of conjugate **7a** with Zn^{2+} together with the calculated isotope pattern for this complex. Additional MS information can be found in the Supporting Information. We were unable to acquire interpretable MS results for Fc conjugates in the presence of Fe^{2+} .

Figure S8 shows the TOF-MS-ES⁺ results of compound **4**, and those of its interaction with Zn^{2+} is shown in Figure S9. First, Zn^{II} can deprotect the trityl group on thiol, for which $m/z = 242.2$, for compound **4** the m/z value is around 647.2, after the removal of trityl group, its m/z value should be 405.0. However, the observed signal at $m/z = 810.0$ (Figure S9) suggests that potentially a dimer is formed after the addition of Zn^{2+} . For compound **5**, the expected m/z is 992.3. Removal of the two trityl groups gives rise to an m/z value of 508.8. This may suggest that Zn^{2+} is able to remove the trityl group from conjugate **5** in solution. However, the same cannot be said for **7a**. The m/z value for compound **6a** is 1266.3, after addition of Zn^{II} and the deprotection of two trityl groups, we obtained $m/z = 484.4$ experimentally, and finally, we got the coordinated compound with molecular weight 845.9. Therefore, Zn^{II} effectively deprotects the trityl groups, which leads to its coordination with the Fc conjugate, but this is not true for compound **7a**; deprotection was carried out by an alternate route shown in Scheme 1. Figure 7 shows a high-resolution mass spectrum of the solution of conjugate **7a**· Zn^{2+} , which displays a peak at $m/z = 561.6$ assigned to $[\text{M} + \text{Zn}]^{2+}$. The

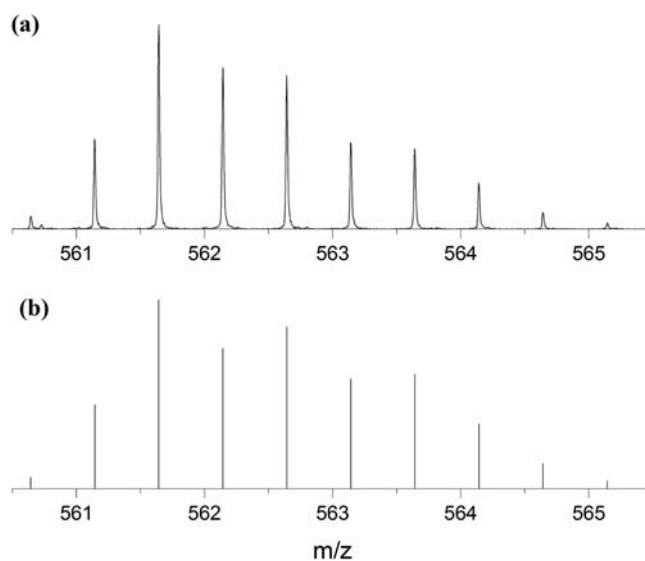


Figure 7. TOF-MS-ES⁺ (positive mode) results showing the experimental and theoretical isotopic pattern of the Zn^{2+} complex conjugate of **7a** assigned to $[\text{M} + \text{Zn}]^{2+}$. (a) Observed partial spectrum of the molecular ion of **7a**· Zn^{2+} in acetonitrile. (b) Calculated isotopic ratio spectrum.

mass spectrum shows an isotope envelope indicative of a Zn complex. Similar results were also observed for compound **7b**· Cd^{2+} , which gave rise to a signal at $m/z = 345.0$ (calculated mass 345.0), showing doubly charged species (Supporting Information). The MS spectra obtained for **7a** and **7b** upon addition of Cd^{2+} showed m/z values of 587.1 and 345.0, correspondingly, which are also indicative of doubly charged species.

Conclusions

In summary, a series of disubstituted Fc-Cys and Fc-His derivatives were successfully synthesized and characterized. These complexes display a quasi-reversible single one-electron oxidation with half-wave potential. All the conjugates under study possess *P*-helical conformation, which was confirmed by CD spectroscopy. Metal coordination to the His-derivatives is feasible, giving rise to distinct metal complexes in which the metal is presumably coordinated to the His imidazole. Interestingly, addition of Zn^{2+} causes a change

in the helicity of conjugates **6a** and **6b** after Zn^{2+} coordination from *P*- to *M*-helical. While we have been unable to obtain single crystals suitable for detailed solid state structural work at this time, we are focusing our attention on obtaining systems that are possible to crystallize in order to obtain more structural information on these systems.

Experimental Section

General Procedure: All syntheses were carried out in air unless otherwise indicated. CH_2Cl_2 (BDH; ACS grade) used for synthesis was dried (CaH_2) and distilled prior to use. CDCl_3 (Aldrich) was dried by and stored over molecular sieves (8–12 mesh; 4 Å effective pore size; Fisher) before use. HBTU, HOBt, H-Cys (Trt or Bzl)-OH (Aldrich), H-His-OMe-2HCl (Aldrich) were used as received, and 1,1'-Fc(COOH)₂ was synthesized. Et_3N (BDH; ACS grade) for the synthesis was used as received. For column chromatography, a column with a width of 2.7 cm (id) and a length of 45 cm was packed 18–22 cm high with 230–400 mesh silica gel (VWR). For TLC, aluminum plates coated with silica gel 60 F254 (EM Science) were used. NMR spectra were recorded with a Mercury-400 spectrometer operating at 400 MHz (^1H) and 125 MHz (^1H , ^{13}C). Peak positions in both ^1H NMR and ^{13}C NMR spectra are reported in ppm relative to TMS. The ^1H NMR spectra are referenced to the residual CHCl_3 signal at $\delta = 7.26$ ppm. All ^{13}C NMR spectra are referenced to the CDCl_3 signal at $\delta = 77.23$ ppm. Mass spectroscopy was carried out with a Finnigan MAT 8200 mass spectrometer. Elemental analysis was carried out with a Vario EL elemental analyzer.

Circular Dichroism: JASCO J-810 was used to analyze the configuration of the complexes and their interaction with metal ions. Solutions (1 mM) of all the compounds were made in dry and distilled acetonitrile for the measurements.

Electrochemical Experiments: All electrochemical experiments were conducted with a glassy carbon working electrode (3 mm), Pt wire was used as counter electrode, and Ag wire was used as reference electrode. IR compensation was applied. Before testing, the glassy carbon electrode was polished with 0.05 μm Al_2O_3 , and then sonicated in MilliQ water for 1 min to fully remove the tiny absorbed Al_2O_3 . It was then rinsed with MilliQ water and dried under a N_2 atmosphere. Pt wire was sonicated and rinsed with ethanol and MilliQ water successively, and then dried under a N_2 atmosphere. Acetonitrile was dried. TBAP (0.1 M in acetonitrile) was used as supporting electrolyte; the scan rate was 100 mV, and the concentration of the compounds was 1.0 mM.

Syntheses and Characterization

(1) Synthesis of Fmoc-Cys(Trt)-His-OMe: Fmoc-Cys(Trt)-OH (1.17 g, 2.0 mmol) was dissolved in dried DCM (100 mL), cooled in an ice bath. Then HOBt (1.2 equiv., 0.32 g, 2.4 mmol) and HBTU (0.91 g, 2.4 mmol) were added immediately. TEA (0.5 mL) was added to dissolve the formed slurry. After stirring for 0.5 h, H-His-OMe-2HCl (0.48 g, 2.0 mmol) in dried DCM (30 mL), together with TEA (0.5 mL), was added dropwise into the first flask over about 10 min. The ice bath was removed, and the mixture was left to stir at room temperature overnight. Then the solution was washed successively with citric acid (10%), saturated sodium hydrogen carbonate, and distilled water. The organic phase was dried with Na_2SO_4 , then filtered and concentrated under reduced pressure in a rotary evaporator to give a white powder of Fmoc-Cys(Trt)-His-OMe (**1**) (1.23 g, 83.5%). ^1H NMR (CDCl_3): $\delta = 7.0$ – 7.8 (m, Fmoc and trityl group), 7.52 (s, 1 H, H-imidazole), 6.70 (s,

1 H, H-imidazole), 6.67 (d, $J = 8.0$ Hz, NH-Fmoc), 5.62 (d, $J = 8.0$ Hz, 1 H, NH-peptide), 4.22 (m, 1 H, CH-His), 4.07 (m, 1 H, CH-Cys), 3.55 (s, 3 H, COOMe), 3.05 (m, 1 H, CH_2 -His), 2.52 (d, $J = 12.0$ Hz, 2 H, CH_2 -Cys) ppm. TOF-MS-ES⁺: calcd. for $\text{C}_{44}\text{H}_{44}\text{N}_4\text{O}_5\text{S}$ 737.3024 [M^+]; found 737.3032.

(2) Synthesis of Ferrocenoyl Cysteine Derivatives: Fc(COOH)₂ (**2**) (0.27 mg, 1.0 mmol) was dissolved in distilled DCM (50 mL), nitrogen-protecting HOBt (0.648 g, 4.8 mmol) and HBTU (1.82 g, 4.8 mmol) were added immediately, and the mixture was stirred overnight. Using an ice bath to cool the mixture down, compound **1** in which the Fmoc group was deprotected by piperidine (1.03 mg, 2.0 mmol) and TEA (1.0 mL) were added sequentially. The reaction mixture was stirred for 2 d until the completion of the reaction. The solution was dried under vacuum and then purified on a flash column, with gradient eluent from chloroform to ethyl acetate/petroleum ether/methanol = 2:1:0.1; compounds **3a** and **3b** were both collected as yellow powders. Compound **3c** was synthesized according to a procedure similar to that of compound **3a**. After deprotection of the trityl group, compound **3d** was obtained. Referring to Scheme 1, compounds **4**, **5**, **6a** and **6b**, **7a**, and **7b** were obtained by using different methods presented in steps ii, iii, iv, v, and vi, correspondingly.

Fe[C₅H₄-CO-Cys(Trt)-OMe][C₅H₄-CO-piperidine] (3a**):** Yield 56.5%, ^1H NMR (CDCl_3 , 298 K): $\delta = 9.17$ (d, $J = 8.0$ Hz, H, NH-Fc), 7.46–7.20 (trityl group), 4.79 (m, 1 H, H-Fc), 4.68 (m, 1 H, H-Fc), 4.64 (m, 1 H, H-Fc), 4.41 (m, 1 H, H-Fc), 4.39 (m, 1 H, H-Fc), 4.36 (m, 1 H, CH-Cys), 4.28 (m, 1 H, H-Fc), 4.24 (m, 1 H, H-Fc), 3.66 (s, 3 H, COOCH₃), 3.60 (m, 2 H, piperidine), 2.86–2.60 (dd, $J = 24.0$, 16.0 Hz, 2 H, CH_2 -Cys), 1.65–1.25 (m, 8 H, piperidine) ppm. ^{13}C NMR (CDCl_3 , 298 K): $\delta = 175.54$, 171.75, 169.07, 144.62, 129.65, 127.91, 126.66, 78.10, 70.88, 70.47, 70.36, 69.93, 69.75, 68.87, 66.94, 52.52, 52.18, 34.11, 33.34 ppm. TOF-MS-ES⁺: calcd. for $\text{C}_{40}\text{H}_{40}\text{N}_2\text{O}_4\text{FeS}$ 700.2058 [M]; found 701.2036 [$\text{M} + \text{H}$]⁺, 723.1956 [$\text{M} + \text{Na}$]⁺, 1423.4024 [$2\text{M} + \text{Na}$]⁺. $\text{C}_{40}\text{H}_{40}\text{FeN}_2\text{O}_4\text{S}$ (700.67): calcd. C 68.25, H 5.31, N 4.21; found C 68.43, H 5.69, N 3.99.

Fe[C₅H₄-CO-Cys(Trt)-His-OMe][C₅H₄-CO-piperidine] (3b**):** Yield 18.2%, ^1H NMR (CDCl_3 , 298 K): $\delta = 9.75$ (d, $J = 8.0$ Hz, 1 H, NH-Fc), 7.62 (s, 1 H, H-imidazole), 7.50–7.17 (trityl group), 6.77 (s, 1 H, H-imidazole), 6.33 (d, $J = 8.0$ Hz, 1 H, NH-peptide), 4.85 (s, 1 H, H-Fc), 4.71 (m, 1 H, CH-His), 4.62 (s, 1 H, H-Fc), 4.58 (s, 1 H, H-Fc), 4.44 (s, 1 H, H-Fc), 4.38 (s, 1 H, H-Fc), 4.31 (s, 1 H, H-Fc), 4.26 (s, 1 H, H-Fc), 4.20 (m, 1 H, H-Fc), 3.73 (s, 3 H, COOCH₃), 3.55 (m, 2 H, piperidine), 3.20–3.00 (dd, $J = 16.0$, 8.0 Hz, 2 H, CH_2 -His), 2.90 (dd, $J = 20.0$, 8.0 Hz, H, CH-Cys), 2.75–2.70 (dd, $J = 12.0$, 8.0 Hz, 2 H, CH_2 -Cys), 1.48–1.25 (m, 8 H, piperidine) ppm. ^{13}C NMR (CDCl_3 , 298 K): $\delta = 172.04$, 170.45, 169.23, 144.55, 129.65, 128.08, 126.83, 82.35, 71.05, 70.16, 70.04, 69.84, 69.09, 68.57, 67.12, 54.61, 53.04, 52.50, 32.55, 31.57 ppm. TOF-MS-ES⁺: calcd. for $\text{C}_{46}\text{H}_{47}\text{N}_5\text{O}_5\text{FeS}$ 837.2647 [M]; found 838.2834 [$\text{M} + \text{H}$]⁺, 1676.4956 [$2\text{M} + \text{H}$]⁺. $\text{C}_{46}\text{H}_{47}\text{FeN}_5\text{O}_5\text{S}$ (837.81): calcd. C 65.55, H 5.81, N 8.56; found C 65.83, H 5.59, N 8.29.

Fe[C₅H₄-CO-Cys(Trt)-Cys(Trt)-His-OMe][C₅H₄-CO-piperidine] (3c**):** Yield 13.3%, ^1H NMR (CDCl_3 , 298 K): $\delta = 9.03$ (d, $J = 8.0$ Hz, 1 H, NH-Fc), 7.49 (s, 1 H, H-imidazole), 7.10–7.15 (trityl group), 6.73 (s, 1 H, H-imidazole), 6.66 (d, $J = 8.0$ Hz, 1 H, NH-peptide), 4.60 (m, 1 H, CH), 4.54 (s, 1 H, H-Fc), 4.46 (m, 1 H, H-Fc), 4.41 (m, 1 H, H-Fc), 4.38 (m, 1 H, H-Fc), 4.25 (m, 1 H, H-Fc), 4.21 (m, 1 H, H-Fc), 4.17 (s, 1 H, H-Fc), 4.01 (m, 2 H, CH-Cys), 3.69 (s, 3 H, COOCH₃), 3.54 (m, 2 H, piperidine), 3.12–2.98 (dd, $J = 16.0$, 8.0 Hz, 2 H, CH_2 -His), 2.83–2.55 (dd, $J = 16.0$, 8.0 Hz, 2 H, CH_2 -Cys), 1.67–1.22 (s, 8 H, piperidine) ppm. ^{13}C

NMR (CDCl₃, 298 K): δ = 177.49, 174.16, 169.11, 167.87, 144.48, 129.54, 127.99, 75.00, 70.41, 69.39, 67.63, 64.97, 64.24, 60.19, 52.60, 52.49, 32.91 ppm. TOF-MS-ES⁺: calcd. for C₆₈H₆₆N₆O₆FeS₂ 1182.3835 [M]; found 1183.3868 [M + H]⁺. C₆₈H₆₆FeN₆O₆S₂ (1183.27): calcd. C 69.31, H 5.21, N 7.30; found C 68.93, H 5.49, N 7.04,

Fe[C₅H₄-CO-Cys-OMe][C₅H₄-CO-piperidine] (3d): Yield 6.1%, ¹H NMR (CDCl₃, 298 K): δ = 9.48 (d, J = 8.0 Hz, H, NH-Fc), 4.84 (m, 1 H, H-Fc), 4.68 (m, 1 H, H-Fc), 4.63 (m, 1 H, H-Fc), 4.43 (m, 1 H, H-Fc), 4.33 (m, H, CH-Cys), 4.29 (m, 1 H, H-Fc), 3.80 (s, 3 H, COOCH₃), 3.60 (m, 2 H, piperidine), 3.08–3.03 (dd, J = 8.0, 4.0 Hz, 2 H, CH₂-Cys), 1.68–1.50 (m, 8 H, piperidine) ppm. ¹³C NMR (CDCl₃, 298 K): δ = 178.10, 171.37, 170.47, 70.82, 70.44, 69.81, 69.02, 55.28, 52.39, 34.67 ppm. TOF-MS-ES⁺: calcd. for C₂₁H₂₆N₂O₄FeS 458.0963 [M]; found 459.0996 [M + H]⁺, 481.0894 [M + Na]⁺. C₂₁H₂₆FeN₂O₄S (458.35): calcd. C 66.51, H 5.14, N 1.95; found C 67.03, H 5.29, N 2.29,

Fe[C₅H₄-CO-Cys(Trt)-OMe][C₅H₄-CO-OMe] (4): Yield 42.5%, ¹H NMR (CDCl₃, 298 K): 7.42–7.19 (trityl group): δ = 6.49 (d, J = 8.0 Hz, H, NH-Fc), 4.92 (m, 1 H, H-Fc), 4.84 (m, 2 H, H-Fc), 4.73 (m, 1 H, CH-Cys), 4.69 (m, 1 H, H-Fc), 4.61 (m, 2 H, H-Fc), 4.48 (m, 1 H, H-Fc), 4.45 (m, 1 H, H-Fc), 4.39 (m, 1 H, H-Fc), 3.79 (s, 3 H, Cys-COOCH₃), 3.75 (s, 3 H, COOCH₃), 2.74 (dd, J = 8.0, 4.0 Hz, 2 H, CH₂-Cys) ppm. ¹³C NMR (CDCl₃, 298 K): δ = 175.78, 171.12, 168.94, 144.29, 129.48, 128.01, 126.88, 73.27, 72.15, 74.47, 66.89, 52.65, 51.87, 33.92 ppm. TOF-MS-ES⁺: calcd. for C₃₆H₃₃NO₅FeS 647.1327 [M]; found 647.1785 [M], 670.1424 [M + Na]⁺. C₃₆H₃₃FeNO₅S (647.57): calcd. C 66.46, H 4.84, N 1.96; found C 66.63, H 5.09, N 2.13,

Fe[C₅H₄-CO-Cys(Trt)-OMe]₂ (5): Yield 33.7%, ¹H NMR (CDCl₃, 298 K): δ = 7.52 (d, J = 8.0 Hz, 2 H, NH-Fc), 7.37–7.16 (trityl group), 4.84 (m, 2 H, H-Fc), 4.74 (m, 2 H, H-Fc), 4.70 (m, 2 H, CH-Cys), 4.50 (m, 2 H, H-Fc), 4.35 (m, 2 H, H-Fc), 3.55 (s, 6 H, COOCH₃), 2.76–2.47 (dd, J = 12.0, 8.0 Hz, 4 H, CH₂-Cys) ppm. ¹³C NMR (CDCl₃, 298 K): δ = 173.26, 170.12, 144.33, 129.50, 127.98, 126.83, 71.94, 71.53, 70.54, 70.21, 52.86, 51.70, 33.18 ppm. TOF-MS-ES⁺: calcd. for C₅₈H₅₂N₂O₆FeS₂ 992.2616 [M]; found 993.2684 [M + H]⁺, 1015.2547 [M + Na]⁺, 2007.5178 [2M + Na]⁺. C₅₈H₅₂FeN₂O₆S₂ (993.03): calcd. C 70.25, H 5.68, N 2.44; found C 70.08, H 5.24, N 2.75,

Fe[C₅H₄-CO-Cys(Trt)-His-OMe]₂ (6a): Yield 11.4%, ¹H NMR (CDCl₃, 298 K): δ = 8.36 (d, J = 8.0 Hz, 2 H, NH-Fc), 7.79 (s, 2 H, H-imidazole), 7.45–7.13 (trityl group), 6.84 (s, 2 H, H-imidazole), 6.52 (d, J = 8.0 Hz, 2 H, NH-peptide), 4.80 (s, 2 H, H-Fc), 4.75 (m, 1 H, CH-His), 4.69 (s, 1 H, H-Fc), 4.54 (s, 1 H, H-Fc), 4.50 (s, 1 H, H-Fc), 4.37 (s, 1 H, H-Fc), 4.35 (s, 1 H, H-Fc), 4.30 (s, 1 H, H-Fc), 4.27 (m, 1 H, H-Fc), 3.82 (s, 6 H, COOCH₃), 3.20 (dd, J = 36.0, 16.0 Hz, 4 H, CH₂-imidazole), 3.15 (dd, J = 16.0, 8.0 Hz, 2 H, CH-Cys), 1.26 (dd, J = 8.0, 4.0 Hz, 4 H, CH₂-Cys) ppm. ¹³C NMR (CDCl₃, 298 K): δ = 176.12, 171.54, 170.82, 144.23, 129.5496, 128.18, 127.01, 71.92, 69.96, 69.41, 67.50, 53.30, 52.63, 31.58 ppm. TOF-MS-ES⁺: calcd. for C₇₀H₆₆N₈O₈FeS₂ 1266.3794 [M]; found 1267.3835 [M + H]⁺. C₇₀H₆₆FeN₈O₈S₂ (1267.31): calcd. C 65.94, H 5.45, N 8.34; found C 66.26, H 5.18, N 8.77,

Fe[C₅H₄-CO-Cys(Bzl)-His-OMe]₂ (6b): Yield 15.7%, ¹H NMR (CDCl₃, 298 K): δ = 8.54 (s, 1 H, NH-Fc), 7.64 (s, 1 H, H-imidazole), 8.04–7.11 (benzyl group), 6.81 (s, 1 H, H-imidazole), 6.58 (d, J = 8.0 Hz, 1 H, NH-peptide), 4.87 (s, 1 H, H-Fc), 4.82 (s, 1 H, H-Fc), 4.77 (m, 1 H, CH-His), 4.72 (s, 1 H, H-Fc), 4.63 (s, 1 H, H-Fc), 4.56 (s, 1 H, H-Fc), 4.42 (s, 1 H, H-Fc), 4.36 (s, 1 H, H-Fc), 4.31 (m, 1 H, H-Fc), 3.77 (s, 3 H, COOCH₃), 3.25–2.65 (dd, J = 36.0, 20.0 Hz, 2 H, CH₂-His; 2 H, dd, CH₂-Cys) ppm. ¹³C NMR

(CDCl₃, 298 K): δ = 176.00, 172.55, 170.93, 143.75, 128.95, 127.33, 72.33, 72.00, 70.60, 68.50, 53.30, 52.77, 36.54 ppm. TOF-MS-ES⁺: C₄₆H₅₀N₈O₈FeS₂ (gmol^{−1}): [M + H]⁺ = 963.2584, [M + 2Cl]⁺ = 1034.1894, cal. [M] = 962.2542. C₄₆H₅₀FeN₈O₈S₂ (962.92): calcd. C 57.08, H 5.13, N 11.24; found C 57.35, H 5.19, N 11.57,

Fe[(C₅H₄-CO)-His(Trt)-OMe]₂ (7a): Yield 67.2%. ¹H NMR (CDCl₃, 298 K): δ = 7.87 (d, J = 7.9 Hz, 2 H, amide NH), 7.36 (d, J = 1.4 Hz, 2 H, H-imidazole), 7.28–7.19 (ddt, J = 12.8, 9.0, 6.0 Hz, 15 H, H-Trt), 6.80 (d, J = 1.4 Hz, 2 H, H-imidazole), 4.92 (m, 2 H, CH-His), 4.89–4.79 (m, 4 H, H-Fc), 4.74–4.24 (m, 6 H, H-Fc), 3.42 (s, 6 H, COOCH₃), 3.21–2.63 (m, 4 H, CH₂-His) ppm. ¹³C NMR (CDCl₃, 298 K): δ = 174.93, 170.04, 142.34, 138.48, 136.28, 129.67, 128.02, 127.95, 120.41, 75.90, 75.20, 72.05, 71.64, 70.31, 70.26, 52.81, 52.46, 29.69 ppm. TOF-MS-ES⁺: calcd. for C₆₄H₅₆N₆O₆Fe 1060.3644 [M]; found 1061.3679 [M + H]⁺. C₆₄H₅₆FeN₆O₆ (1061.03): calcd. C 72.45, N 7.92; found C 72.31, N 8.14. ¹H NMR ([D₃]acetonitrile): δ = 8.07 (d, J = 7.5 Hz, 2 H, amide NH), 7.51 (br. s, 2 H, H-imidazole), 7.41–7.11 (m, J = 4.0, 2.0 Hz, 15 H, H-Trt), 7.14 (m, 15 H, H-Trt), 6.78 (d, J = 1.4 Hz, 2 H, H-imidazole), 4.67 (m, J = 5.6, 2.6, 1.3 Hz, 4 H, H-Fc), 4.61 (m, J = 7.5, 5.0 Hz, 2 H, CH-His), 4.49 (m, J = 2.6, 1.4 Hz, 2 H, H-Fc), 4.41 (m, J = 2.5, 1.2 Hz, 2 H, H-Fc), 3.55 (s, 6 H, COOCH₃), 2.93 (m, J = 6.4 Hz, 4 H, CH₂-His) ppm. ¹³C NMR (CD₃CN, 298 K): δ = 173.12, 169.28, 142.58, 138.55, 136.78, 129.50, 128.11, 127.97, 119.83, 76.93, 75.04, 72.20, 71.70, 70.13, 69.59, 52.98, 51.88, 29.07 ppm.

Fe[(C₅H₄-CO)-His-OMe]₂ (7b): Yield 97.2%. ¹H NMR ([D₃]acetonitrile): δ = 8.54 (s, 2 H, H-imidazole), 7.94 (d, J = 8.1 Hz, 2 H, amide NH), 7.39 (s, 2 H, H-imidazole), 4.94 (td, J = 9.4, 9.0, 4.2 Hz), 4.53 (dd, J = 101.2, 31.0 Hz, 8 H, H-Fc), 3.77 (s, 6 H, COOCH₃), 3.47–3.24 (m, J = 32.7, 6.8 Hz, 4 H, CH₂-His) ppm. ¹³C NMR (CD₃CN, 298 K): δ = 173.18, 169.325, 142.57, 138.54, 136.75, 129.49, 128.11, 127.98, 119.86, 76.88, 75.03, 72.21, 71.71, 70.13, 69.59, 52.98, 51.91, 29.04 ppm. TOF-MS-ES⁺: calcd. for C₂₆H₂₈N₆O₆Fe 577.1492 [M + 1]⁺; found 577.1438 [M + H]⁺. C₂₆H₂₈FeN₆O₆ (576.39): calcd. C 54.18, N 14.58; found C 54.05, N 14.39,

Supporting Information (see footnote on the first page of this article): ¹H NMR spectra for all compounds, NMR spectroscopic titration experiments, CD spectra, CV data and plots, MS spectra before and after metal addition.

Acknowledgments

The authors gratefully acknowledge the financial support by the National Science and Engineering Research Council of Canada, the National Nature Science Foundation of China (Nos. 61301038, 61271119), and the University of Toronto.

- [1] G. Bulaj, T. Kortemme, D. P. Goldenberg, *Biochemistry* **1998**, *37*, 8965–8972.
- [2] X. Chen, S. K. Ko, M. J. Kim, I. Shin, J. Yoon, *Chem. Commun.* **2010**, *46*, 2751–2753.
- [3] R. Lill, U. Muhlenhoff, *Annu. Rev. Cell Dev. Biol.* **2006**, *22*, 457–486.
- [4] J. Ballmann, A. Albers, S. Demeshko, S. Dechert, E. Bill, E. Bothe, U. Ryde, F. Meyer, *Angew. Chem. Int. Ed.* **2008**, *47*, 9537–9541; *Angew. Chem.* **2008**, *120*, 9680.
- [5] T. Iwasaki, A. Kounosu, D. R. J. Kolling, S. Lhee, A. R. Crofts, S. A. Dikanov, T. Uchiyama, T. Kumasaka, H. Ishikawa, M. Kono, T. Imai, A. Urushiyama, *Protein Sci.* **2006**, *15*, 2019–2024.

- [6] A. J. Fielding, K. Parey, U. Ermler, S. Scheller, B. Jaun, M. Bennati, *J. Biol. Inorg. Chem.* **2013**, *52*, 905–914.
- [7] E. Denke, T. Merbitz-Zahradnik, O. M. Hatzfeld, C. H. Snyder, T. A. Link, B. L. Trumpower, *J. Biol. Chem.* **1998**, *273*, 9085–9093.
- [8] E. Cotner-Gohara, L. K. Kim, M. Hammel, J. A. Tainer, A. E. Tomkinson, T. Ellenberger, *Biochemistry* **2010**, *49*, 6165–6176.
- [9] E. T. Chouchani, T. R. Hurd, S. M. Nadtochiy, P. S. Brookes, I. M. Fearnley, K. S. Lilley, R. A. J. Smith, M. P. Murphy, *Biochem. J.* **2010**, *430*, 47–59.
- [10] R. D. Bach, *J. Phys. Chem. C* **2010**, *114*, 9319–9332.
- [11] V. Fourmond, P. Infossi, M. T. Giudici-Orticoni, P. Bertrand, C. Leger, *J. Am. Chem. Soc.* **2010**, *132*, 4848–4857.
- [12] D. H. Baker, G. L. Czarnecki-maulden, *J. Nutr.* **1987**, *117*, 1003–1010.
- [13] H. Cao, M. Wei, Z. Chen, Y. Huang, *Analyst* **2013**, *138*, 2420–2426.
- [14] F. Jalilehvand, K. Parmar, S. Zielke, *Metallomics* **2013**, *5*, 1368–1376.
- [15] B. O. Leung, F. Jalilehvand, V. Mah, *Dalton Trans.* **2007**, *41*, 4666–4674.
- [16] V. Mah, F. Jalilehvand, *J. Biol. Inorg. Chem.* **2008**, *13*, 541–553.
- [17] V. Mah, F. Jalilehvand, *Chem. Res. Toxicol.* **2010**, *23*, 1815–1823.
- [18] L. Patrick, *Altern. Med. Rev.* **2003**, *8*, 106–128.
- [19] G. Bertin, D. Averbeck, *Biochimie* **2006**, *88*, 1549–1559.
- [20] C. T. McMurray, J. A. Tainer, *Nat. Genet.* **2003**, *34*, 239–241.
- [21] A. Hartwig, *Antioxid. Redox Signaling* **2001**, *3*, 625–634.
- [22] U. Wimmer, Y. Wang, O. Georgiev, W. Schaffner, *Nucleic Acids Res.* **2005**, *33*, 5715–5727.
- [23] F. Jalilehvand, B. O. Leung, V. Mah, *Inorg. Chem.* **2009**, *48*, 5758–5771.
- [24] F. Jalilehvand, V. Mah, B. O. Leung, J. Mink, G. M. Bernard, L. Hajba, *Inorg. Chem.* **2009**, *48*, 4219–4230.
- [25] F. Jalilehvand, Z. Amini, K. Parmar, E. Y. Kang, *Dalton Trans.* **2011**, *40*, 12771–12778.
- [26] F. Jalilehvand, Z. Amini, K. Parmar, *Inorg. Chem.* **2012**, *51*, 10619–10630.
- [27] E. Hoch, W. Lin, J. Chai, M. Hershfinkel, D. Fu, I. Sekler, *Proc. Natl. Acad. Sci. USA* **2012**, *109*, 7202–7207.
- [28] L. Fairall, J. W. R. Schwabe, L. Chapman, J. T. Finch, D. Rhodes, *Nature* **1993**, *366*, 483–487.
- [29] J. M. Berg, Y. Shi, *Science* **1996**, *271*, 1081–1085.
- [30] J. P. Mackay, M. Crossley, *Trends Biochem. Sci.* **1998**, *23*, 1–4.
- [31] G. G. Briand, N. Burford, *Chem. Rev.* **1999**, *99*, 2601–2657.
- [32] P. J. Sadler, H. Li, H. Sun, *Coord. Chem. Rev.* **1999**, *185–186*, 689–709.
- [33] G. G. Briand, N. Burford, M. D. Eelman, N. Aumeerally, L. Chen, T. S. Cameron, K. N. Robertson, *Inorg. Chem.* **2004**, *43*, 6495–6500.
- [34] N. Burford, M. D. Eelman, D. E. Mahony, M. Morash, *Chem. Commun.* **2003**, *7*, 146–147.
- [35] H. A. Phillips, M. D. Eelman, N. Burford, *J. Inorg. Biochem.* **2007**, *101*, 736–739.
- [36] V. Edwards-Jones, *Lett. Appl. Microbiol.* **2009**, *49*, 147–152.
- [37] B. S. Atiyeh, M. Costagliola, S. N. Hayek, S. A. Dibo, *Burns* **2007**, *33*, 139–148.
- [38] O. Gordon, T. V. Slenters, P. S. Brunetto, A. E. Villaruz, D. E. Sturdevant, M. Otto, R. Landmann, K. M. Fromm, *Antimicrob. Agents Chemother.* **2010**, *54*, 4208–4218.
- [39] B. O. Leung, F. Jalilehvand, V. Mah, M. Parvez, Q. Wu, *Inorg. Chem.* **2013**, *52*, 4593–4602.
- [40] a) D. R. van Staveren, N. Metzler-Nolte, *Chem. Rev.* **2004**, *104*, 5931–5986; b) T. Moriuchi, T. Hirao, *Acc. Chem. Res.* **2010**, *43*, 1040–1051.
- [41] a) F. E. Appoh, T. C. Sutherland, H.-B. Kraatz, *J. Organomet. Chem.* **2005**, *690*, 1209–1217; b) S. Chowdhury, G. Schatte, H.-B. Kraatz, *Eur. J. Inorg. Chem.* **2006**, 988–993; c) B. Adhikari, A. J. Lough, B. Barker, A. Shah, C. Xiang, H.-B. Kraatz, *Organometallics* **2014**, DOI: 10.1021/om500032p; d) X. de Hatten, E. Bothe, K. Merz, I. Huc, N. Metzler-Nolte, *Eur. J. Inorg. Chem.* **2008**, 4530.
- [42] a) L. Barisic, M. Cakic, K. A. Mahmoud, Y.-N. Liu, H.-B. Kraatz, H. Pritzkow, N. Metzler-Nolte, S. I. Kirin, V. Rapić, *Chem. Eur. J.* **2006**, *12*, 4965–4980 and references cited therein; b) S. Kirin, H.-B. Kraatz, N. Metzler-Nolte, *Chem. Soc. Rev.* **2006**, *35*, 348–354.
- [43] a) H. Kessler, *Angew. Chem. Int. Ed. Engl.* **1982**, *21*, 512–523; *Angew. Chem.* **1982**, *94*, 509; b) S. H. Gellman, G. P. Dado, G. B. Liang, B. R. Adams, *J. Am. Chem. Soc.* **1991**, *113*, 1164; c) K. Y. Tsang, H. Diaz, N. Graciani, J. W. Kelly, *J. Am. Chem. Soc.* **1994**, *116*, 3988.
- [44] T. Moriuchi, A. Nomoto, K. Yoshida, A. Ogawa, T. Hirao, *J. Am. Chem. Soc.* **2001**, *123*, 68–75.
- [45] R. S. Herrick, R. M. Jarret, T. P. Curran, D. R. Dragoli, M. B. Flaherty, S. E. Lindyberg, R. A. Slate, L. C. Thornton, *Tetrahedron Lett.* **1996**, *37*, 5289–5292.
- [46] a) S. I. Kirin, D. Wissenbach, N. Metzler-Nolte, *New J. Chem.* **2005**, *29*, 1168–1173; b) X. de Hatten, T. Weyermüller, N. Metzler-Nolte, *J. Organomet. Chem.* **2004**, *689*, 4856–4867.
- [47] M. Kawai, U. Nagai, Y. Inai, H. Yamamura, R. Akasaka, S. Takagi, Y. Miwa, T. Taga, *Pept. Sci.* **2005**, *80*, 186–198.
- [48] H. Lavanant, E. Hecquet, Y. Hoppilliard, *Int. J. Mass Spectrom.* **1999**, *187*, 11–23.

Received: May 26, 2014

Published Online: September 17, 2014